

Rotational Reconstruction of Sapphire (0001)

Igor Vilfan,^a Frédéric Lançon^b and Jacques Villain^b

^a*J. Stefan Institute, P.O. Box 3000, SI-1001 Ljubljana, Slovenia*

e-mail: igor.vilfan@ijs.si

^b*Département de Recherche Fondamentale sur la Matière Condensée,*

CEA-Grenoble, F-38054 Grenoble cedex 9, France

PACS numbers: 68.35 Bs, 68.35 Md, 61.50 Ah, 68.10 Jy

Abstract

The structure of the $(\sqrt{31} \times \sqrt{31})R \pm 9^\circ$ reconstructed phase on sapphire (0001) surface is investigated by means of a simulation based on the energy minimization. The interaction between Al adatoms is described with the semi-empirical many-body Sutton-Chen potential, corrected for the charge transfer between the metallic overlayer and the substrate. The interactions between the Al adatoms and sapphire substrate are described with a simple three-dimensional potential field which has the hexagonal periodicity of sapphire surface. Our energy analysis gave evidence that the structure which is observed at room temperature is in fact a frozen high-temperature structure. In accordance with the X-ray scattering, a hexagonal domain pattern separated by domain walls has been found. The Al adatoms, distributed in two monolayers, are ordered and isomorphic to metallic Al(111) in the domains and disordered in the domain walls. The main reason for the rotational reconstruction is the lattice misfit between the metallic Al and sapphire.

Key words: Surface relaxation and reconstruction. Sapphire. Surface thermodynamics. Computer simulations.

1 Introduction

Sapphire $\alpha\text{-Al}_2\text{O}_3$ is a technologically important material with a variety of (0001) surface reconstructions. Upon heating in UHV, the nonreconstructed (1×1) surface is stable up to ~ 1250 C. Above this temperature, oxygen gradually evaporates whereas Al stays on the surface [1]. As a consequence, the surface first reconstructs to $(\sqrt{3} \times \sqrt{3})$ rotated by 30° (or (2×2) , as reported by Gautier et al [4]), then to $(3\sqrt{3} \times 3\sqrt{3})$ rotated by 30° and finally, after ~ 20 minutes at 1350 C, to the $(\sqrt{31} \times \sqrt{31})R \pm 9^\circ$ structure [1,2]. It is this last reconstruction which will be the subject of the present paper. The LEED pattern was first investigated by French and Somorjai [1] who found a cubic Al-rich surface structure over the hexagonal-symmetry bulk. More recently, Vermeersch et al. [3] obtained the same reconstruction after evaporating up to ~ 2 ML of Al on clean non-reconstructed sapphire surface. Gautier et al. [4] measured the electron energy loss spectra and found a small hump in the sapphire band gap region. This hump is an indication of metallic character of the Al-rich surface layer. Renaud et al. [2] made very precise grazing-incidence X-ray diffraction (GIXD) measurements and were the first to propose a possible atomic structure of the $(\sqrt{31} \times \sqrt{31})$ structure. However, the Fourier transform of the GIXD provides the Patterson map and not the real-space atomic structures. The lateral positions of Al atoms in the disordered regions could not be uniquely determined. In addition, the GIXD measurements could not tell the altitude of individual atoms above the substrate. Nevertheless, Renaud et al. [2] found that the Al overlayer forms a hexagonal domain pattern. Al atoms are ordered in two compact (111) planes of an FCC lattice, characteristic of metallic Al monolayers, within the domains and highly disordered in the “domain walls” between them. Whereas the origin of the domain pattern was attributed to the lattice misfit between Al overlayer and the substrate,

the reason for the $\pm 9^\circ$ rotation was less clear.

Interestingly enough, evaporation of two topmost planes of oxygens from sapphire crystal leaves behind 5 Al atoms per surface unit cell, very close to the density observed by Renaud et al. [2].

A mechanism of rotational reconstruction was proposed theoretically by Novaco and McTague [5] and confirmed experimentally for several systems, including rare gases (physisorbed) and alkali metals (chemisorbed) on graphite [6,7] and metals on metals [8,9]. In the Novaco and McTague model, rotational reconstruction was attributed to lattice misfit combined with weak coupling between the overlayer and the substrate. This caused a weak sinusoidal lateral distortion of the overlayer lattice. Interestingly enough, rotational reconstruction was observed for lattice misfits as large as 15 % [8].

Rotational reconstruction on sapphire, on the other hand, is different and cannot be completely explained by the Novaco-McTague model. The origin of the reconstruction is still the lattice misfit between the overlayer and the substrate, but now the distortion seems to be so strong that some atoms in the domain walls have lower coordination. This strong disorder could be the consequence of strong overlayer–substrate interactions and not of large lattice misfit. For the $(\sqrt{31} \times \sqrt{31})$ reconstruction the misfit between the sapphire bulk and the Al metal overlayer is only ~ 4 % and is substantially less than in some other rotationally reconstructed systems [8]. On the other hand, the interaction is strong also for some other rotationally reconstructed systems like Cs chemisorbed on graphite [7]. There is another important difference between the reconstructed sapphire and other systems: the overlayer on sapphire is composed of two monolayers [2] whereas in the other systems, it is composed of only one monolayer. Evidently, the origin of rotational reconstruction and

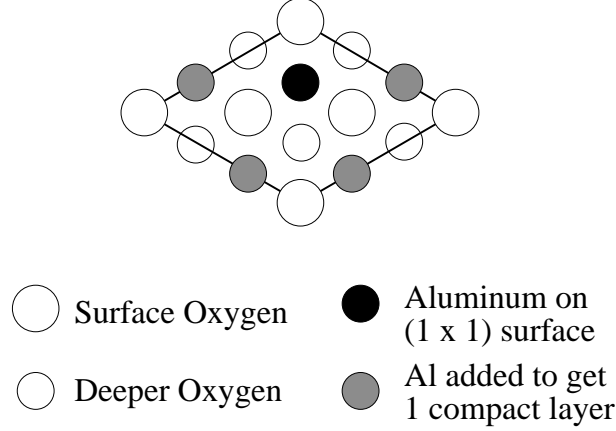


Fig. 1. Unit cell of non-reconstructed sapphire (0001). Al atoms (black circles) in the topmost plane are followed by an oxygen plane (open circles). Al atoms in the bulk of sapphire are not displayed whereas the next oxygen layer is shown with smaller open circles. Upon evaporation of oxygen, the density of surface Al atoms increases. Shaded circles represent added Al atoms if sapphire were covered with one compact in-register Al monolayer.

of strong disorder in the domain walls is not clear.

In this paper we report on a simulation of the $(\sqrt{31} \times \sqrt{31})$ rotational reconstruction of sapphire with the aim of better understanding the processes of rotational reconstruction on the sapphire and similar surfaces and to help resolve some of the above open questions.

2 The Model

The unit cell of clean, nonreconstructed sapphire (0001) surface is shown in Fig. 1. It is terminated with an Al plane with one Al atom per surface unit cell (black disc; 1/3 of a compact monolayer (ML) coverage) [10]. Also shown (shaded discs) are Al atoms which have to be added to get one unexpanded compact monolayer, in register with sapphire.

The reconstructed surface unit cell has about 157 Al atoms in the overlayer [2], so one has to simulate rather large surface unit cells. This is possible only with efficient potentials, therefore we describe the interaction between the overlayer atoms with the semi-empirical Sutton-Chen potential [11,12] which has been also used in studying surface properties, including reconstruction, of FCC metals [13]. These potentials are many-body potentials with elements of two-body terms in it and are written in the form:

$$U = \frac{1}{2} \sum_{i \neq j} \epsilon \left(\frac{a}{r_{ij}} \right)^n - \epsilon C \sum_i \sqrt{\rho_i} \quad (1)$$

(r_{ij} is the separation between the atoms i and j). The first term in (1) represents the core repulsion potential and the second term the bonding energy mediated by the electrons. ρ_i is an effective local electron density at the site i and is written as:

$$\rho_i = \sum_{j \neq i} \left(\frac{a}{r_{ij}} \right)^m. \quad (2)$$

ϵ and C are parameters of the model which, together with the exponents n and m , determine the repulsive and cohesive energies, respectively. a is the lattice constant of an Al FCC crystal. Sutton and Chen [11] published the following values for the potential parameters of Al:

$$m = 6, \quad n = 7, \quad \epsilon = 33.147 \text{ meV}, \quad \epsilon C = 16.399 \text{ meV}. \quad (3)$$

We truncated the potential continuously (with a fifth order polynomial) between $r/r_0 = 3.17$ and 3.32 (r_0 is the nearest-neighbour distance). In this way the cutoff is between the 10th and 11th shells of neighbours. That meant that interaction with 68 neighbours were included if Al were perfectly ordered in two FCC(111) planes. With this set of parameters, the cohesive energy in the bulk Al is 3.313 eV/atom, compared to 3.34 eV/atom in [11]. The difference

comes from different cutoff radii.

The origin of bonding is in the electrons of the overlayer. On the reconstructed surface, there are about 5 Al atoms per nonreconstructed unit cell, on the average. Each Al atom has two $3s$ and one $3p$ electrons which all contribute to the cohesive energy. Out of these 5 atoms, one is already present on the non-reconstructed surface and is ionically bound to the sapphire substrate. This reduces the effective density of the electrons in the conduction band by $1/5$ and thus scales the constant ϵC in equation (1) by a factor $\sqrt{4/5}$ (*i.e.*, $\epsilon C = 14.668$ eV). ϵC can be additionally reduced by the charge transfer between the metallic overlayer and the insulating substrate [4]. It is not known how strong the charge transfer is, therefore we treated the constant C as an adjustable parameter.

The interaction between the overlayer and the substrate was modelled by a simple periodic potential. The substrate is much stiffer than the Al overlayer, therefore the relaxation of the substrate caused by the overlayer was neglected in the simulations. The substrate potential was expanded in a power series and only the six lowest-order terms were retained, similarly as in the studies of noble gases on graphite,

$$U_S = \frac{U_L - \cos(\vec{k}_1 \cdot \vec{r}) \cos(\vec{k}_2 \cdot \vec{r}) \cos(\vec{k}_3 \cdot \vec{r})}{U_L - 1} U_{LJ}(z). \quad (4)$$

$$\vec{k}_1 = \frac{2\pi}{a_s}(0, 1), \quad \vec{k}_2 = \frac{\pi}{a_s}(\sqrt{3}, -1), \quad \vec{k}_3 = \frac{\pi}{a_s}(-\sqrt{3}, -1) \quad (5)$$

are the unit vectors in the plane of the surface, and a_s the substrate lattice constant. U_L controls the lateral modulation of the potential, and U_{LJ} ,

$$U_{LJ}(z) = U_0 \left[\left(\frac{z_0}{z} \right)^{12} - 2 \left(\frac{z_0}{z} \right)^6 \right], \quad (6)$$

its z -dependence, in the direction perpendicular to the surface. This depen-

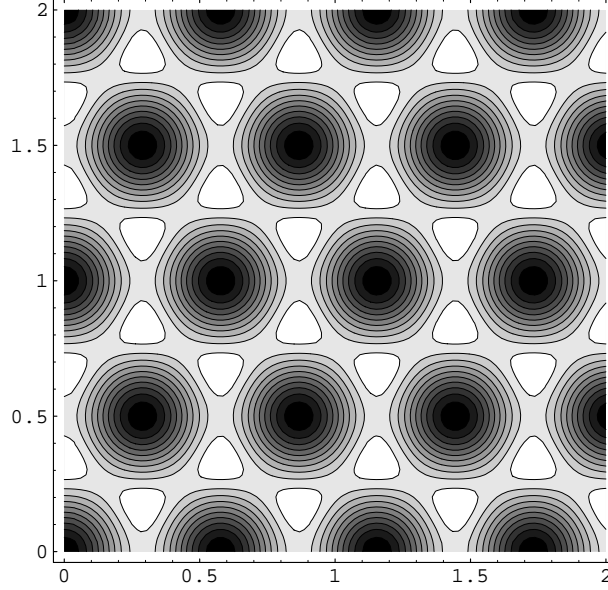


Fig. 2. The substrate potential has six equally deep minima (white) around each maximum (black) which is located above the last layer of oxygens.

dence is necessary because the overlayer is more than one monolayer thick. In the Lennard-Jones potential (6), U_0 is the depth of the substrate potential and z_0 determines the position of the minimum and the width of the potential in the vertical direction. Thus, the overlayer – substrate potential is described by three variational parameters, U_L , U_0 , and z_0 . This potential, shown in Fig 2, has six equally deep minima around each topmost oxygen atom of sapphire substrate. The potential (4) is not deeper on the sites, already occupied by Al atoms on the unreconstructed (0001) surface. This simplification is backed by a careful inspection of the real-space overlayer structure obtained from the diffraction data [2]. During the process of reconstruction, the original Al atoms also moved to other positions. They are not stronger bound than any other Al atoms coming to the surface during oxygen evaporation.

We simulated a box with the base plane of $\sqrt{93}a \times \sqrt{31}a$. Such a rectangle accommodates exactly two reconstructed surface unit cells under periodic

boundary conditions for the overlayer and substrate. The in-plane symmetry axis of the substrate is rotated with respect to the rectangle by $\alpha = \sin^{-1}(\sqrt{93}/62) \approx 8.9^\circ$. In the initial configurations the Al atoms were put on two planes and positioned close to the positions found by Renaud et al. [2]. We started with this configuration because of the problems with metastability.

Our results have been compared with the GIXD result of Renaud et al. [2] who found 157 adatoms in a surface unit cell, distributed in two monolayers. In their analysis, however, some atomic sites could have been only partially occupied. Therefore we performed simulations with the number of Al atoms in the overlayer varying from 302 to 318 adatoms (in two unit cells).

For a given set of the potential parameters C , U_L , U_0 and z_0 , the equilibrium Al atomic positions were calculated by the energy minimization. Once the atomic positions were determined, we calculated the corresponding diffraction pattern, given by the structure factors $S_c(\vec{Q})$ of the Bragg peaks at $\vec{Q} = (h, k)$, and compared it with the experimental $S_e(\vec{Q})$ [2,15]. To evaluate the quality of the fit we first scaled $S_c(\vec{Q})$ with a factor s and then calculated the residue, introduced as

$$\chi^2 = \frac{\sum_Q [S_e(\vec{Q}) - sS_c(\vec{Q})]^2}{\sum_Q [S_e(\vec{Q})]^2}. \quad (7)$$

The scaling factor s was chosen to minimise the residue χ^2 :

$$s = \frac{\sum_Q [S_e(\vec{Q})S_c(\vec{Q})]}{\sum_Q [S_c(\vec{Q})]^2}. \quad (8)$$

Summation over the first 17×16 nonequivalent diffraction peaks in the reciprocal space was performed. The parameters C , U_L , U_0 and z_0 were then varied to find the minimal χ^2 .

In the process of relaxation towards the (local) minimum energy configura-

tion with the lowest residue, severe problems with hysteresis and local energy minima (metastability) were encountered. This is not too surprising since the “domain wall” region is full of lattice defects. To avoid trapping in a metastable state, the relaxed structure was shaken randomly and relaxed again.

3 Results

The best agreement between the calculated and experimental diffraction patterns was found, and the most extensive simulations have been done for the structure with 314 adatoms (157 per reconstructed surface unit cell). The best fit between with 314 atoms was obtained for

$$\epsilon C = 13.87\text{eV} \quad U_L = 4.56 \quad U_0 = 1.35\text{eV} \quad z_0 = 2.64\text{\AA}. \quad (9)$$

The energy of this structure is $E = -3.21$ eV/adatom. The average core repulsion energy between the adatoms is 1.65 eV, the bonding energy between them is -3.95 eV, and the average interaction energy with the substrate is -0.92 eV.

The real-space structure with the best fit is seen in Fig. 3. Comparison of the real-space structures obtained from the simulation and from the GIXD shows that the simulated structure is substantially more ordered and that the simulated disordered regions, domain walls are broader and less pronounced. The two domains in the simulated box do not have the same structure after relaxation although their initial configurations were identical. This is an indication of many metastable states in the disordered regions.

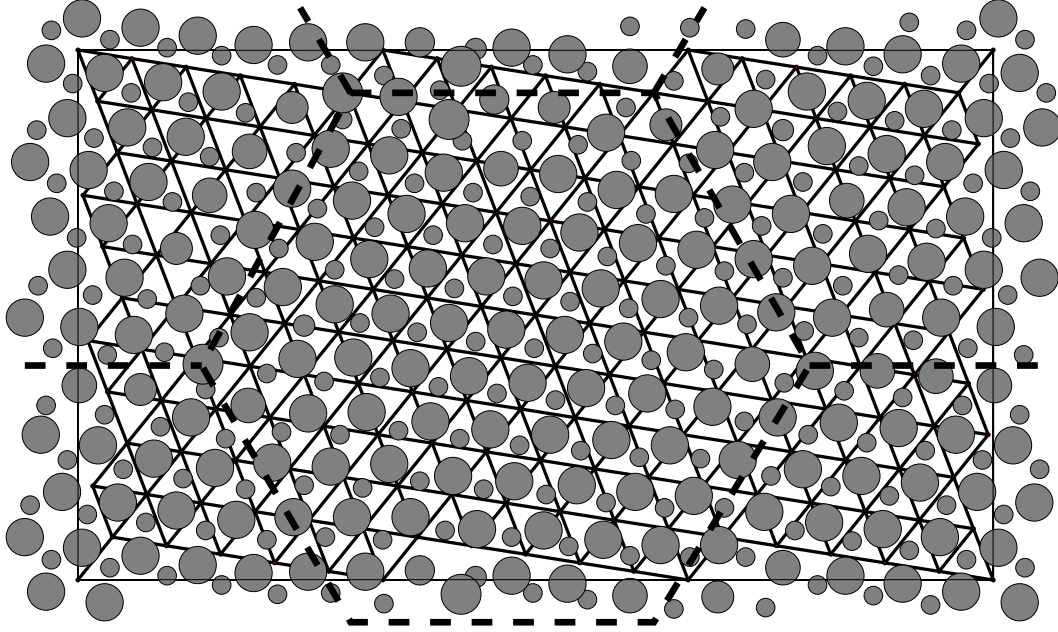


Fig. 3. Structure of the Al overlayer obtained in the simulation of 314 atoms in a rectangle of the size $\sqrt{93}a \times \sqrt{31}a$ with periodic boundary conditions. The corners of the underlying triangles show the positions of the topmost oxygens of sapphire, where the substrate potential is maximal. The potential is minimal in the centres of the triangles. The grey circles represent the Al atoms and their radii are proportional to the altitude of the atom above the substrate. The Al atoms are arranged in two monolayers, the larger circles show the atoms in the upper layer and the smaller circles the atoms of the lower layer. The atoms are more ordered and closer to the minima of the substrate potential in the hexagonal domains and more disordered close to the walls (dashed lines) separating the domains. Notice that the two domains do not have the same structure in the disordered regions.

The residue can be compared with the experimental uncertainty σ , defined as

$$\sigma^2 = \frac{\sum_Q [\sigma(\vec{Q})]^2}{\sum_Q [S_e(\vec{Q})]^2}, \quad (10)$$

where $\sigma(\vec{Q})$ are the experimental uncertainties of the structure factors at the Bragg points \vec{Q} . Using the experimental data of Renaud [15], we found $\sigma =$

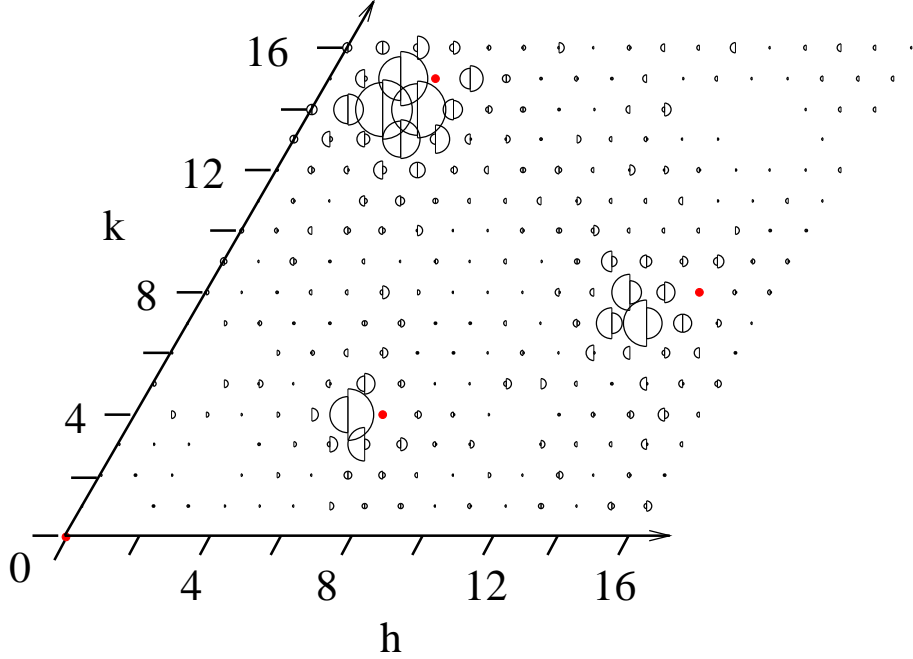


Fig. 4. Calculated (left-hand semicircles) and experimental (right-hand semicircles) [2] diffraction patterns, indexed in the reciprocal space of the reconstructed surface unit cell. Small black disks are the bulk allowed reflections.

0.28 whereas our best fit had $\chi = 0.5$. Comparison of the calculated and experimental structure factors, Fig. 4 shows good agreement of the intense peaks around the substrate Bragg peaks. Some discrepancy is observed for less intense peaks further away from the substrate Bragg peaks. The biggest difference in the structure factors is found for $\vec{Q} = (7, 3)$. The reason is most probably in the simple substrate potential used, so one cannot expect to find exactly the same structure as on a real sapphire surface.

4 Discussion

The simulations were done by energy minimization. In principle, however, the energy minimization is acceptable only for low temperatures, when the entropy is small, and one should minimize the free energy. It is expected that

the structure observed in the experiment at room temperature has minimal free energy at the freezing temperature which is substantially higher than the room temperature. At the freezing temperature, the contribution of the entropy is significant. This – together with the simplified overlayer-substrate potential – possibly explains why the more disordered structure with the best fit has higher energy than some other – more ordered – structures with worse fit. Indeed, the energy difference between different structures, simulated with the same variational parameters, was of the order 0.01 eV/atom (if distributed uniformly among 314 atoms) and is of the same order as the contribution of the entropy to the free energy at the freezing temperature.

Another mechanism which would lead to a metastable overlayer structure could be channeling, transport of Al atoms directly into a strongly metastable state on the surface during the process of oxygen evaporation. However, it is very unlikely that the metastable potential minima would be so deep that diffusion at ~ 1000 K couldn't bring the overlayer structure to an equilibrium.

Renaud et al. were not able to tell in their paper [2] which Al plane is higher. They did, however, distinguish between the more ordered and more disordered planes. On the basis of preliminary numerical relaxation they anticipated that the more disordered layer was the lower plane. Our simulation does not support this distinction, we found both planes equally disordered.

if the simulations were done with 314 Al atoms, 158 atoms were found in the lower layer, which is much flatter than the upper layer. In the hexagonal domains, the Al atoms are well ordered in both planes like in metallic Al(111). In the domain walls, the Al atoms are strongly disordered. In the simulation, the disorder is manifested also in such a way that equivalent atoms in different reconstructed unit cells had different positions, the translational symmetry of

the reconstructed unit cell was broken.

Simulations with different number of Al atoms, N_{Al} , show a strong increase in χ if $N_{Al} > 314$ and a small increase if $N_{Al} < 314$. For $N_{Al} > 314$, Al atoms very often moved into the third plane.

In our “best fit” structure, Fig. 3, the disordered regions (domain walls) were less pronounced than in the structure proposed by Renaud et al. [2]. Our structure has a smoother transition between the domains, one could say that our domain walls are broader. It is not clear to which extent this difference is the consequence of approximate description of the substrate potential.

With the substrate potential described by Eq. (4), one cannot study the process of oxygen evaporation, we cannot say whether two overlayers of Al are stable or only a transient state and more Al layers are formed upon further heating. A stabilizing mechanism, discussed in detail by Chen et al. [16], is based on the attraction between two surfaces across a thin metal, similar to the Casimir effect. This attraction is described by the Hamaker constant. We estimated the Hamaker constant of Al metal between sapphire insulator and vacuum, $H \approx -3.7 \times 10^{-2}$ eV. The corresponding energy gain is of the order 10^{-3} eV/(Al atom). We conclude that this mechanism of attraction between the two adjacent interfaces is too weak to stop the overlayer growth at two monolayers. In fact, the experimentalists observe that further heating in UHV brings more Al atoms to the surface [15], the two-layer $(\sqrt{31} \times \sqrt{31})R \pm 9^\circ$ reconstructed structure is thus not an equilibrium state of sapphire at 1350 C. Thus, in UHV, more Al atoms build next monolayers whereas heating under oxygen atmosphere oxidizes and deconstructs the surface.

The fact that a metallic type potential, Eq. (1), leads to a good model of this reconstructed sapphire surface is consistent with the metallic character of its

Al overlayer. The minor discrepancy in some diffraction peaks is probably due to the oversimplified substrate potential which cannot lead to the exact details of the reconstruction. But the good overall agreement of the diffraction patterns shows that we have used reasonable interatomic interaction ingredients to simulate this reconstruction.

Acknowledgements

The authors are indebted to G. Renaud for many interesting discussions and for providing them his experimental results. The financial support of the French-Slovenian programme Proteus is deeply acknowledged.

References

- [1] T. M. French and G. A. Somorjai, J. Phys. Chem. **74**, 2489 (1970).
- [2] G. Renaud, B. Villette, I. Vilfan, and A. Bourret, Phys. Rev. Lett. **73**, 1825 (1994).
- [3] M. Vermeersch, R. Sporken, P. Lambin, and R. Caudano, Surf. Sci. **235**, 5 (1990).
- [4] M. Gautier, J. P. Duraud, L. Pham Van, and M. J. Guittet, Surf. Sci. **250**, 71 (1991).
- [5] A. D. Novaco and J. P. McTague, Phys. Rev. Lett. **38**, 1286 (1977); J. P. McTague and A. D. Novaco, Phys. Rev. B **19**, 5299 (1979).
- [6] C. G. Shaw, S. C. Fain, Jr., and M. D. Chinn, Phys. Rev. Lett. **41**, 955 (1978).
- [7] N. J. Wu, Z. P. Hu, and A. Ignatiev, Phys. Rev. B **43**, 3805 (1991).

- [8] M. F. Toner et al., Phys. Rev. B **42**, 5594 (1990).
- [9] D. Fisher and R. D. Diehl, Phys. Rev. B **46**, 2512 (1992).
- [10] P. W. Tasker, Adv. Ceram. **10**, 176 (1988); I. Manassidis, A. De Vita, and M. J. Gillan, Surf. Sci. Lett. **285**, L517 (1993).
- [11] A. P. Sutton and J. Chen, Phil. Mag. Lett. **61**, 139 (1990).
- [12] M. W. Finnis and J. E. Sinclair, Phil. Mag. A **50**, 45 (1984).
- [13] B. D. Todd and R. M. Lynden-Bell, Surf. Sci. **281**, 191 (1993).
- [14] N. W. Ashcroft and N. D. Mermin, *Solid State Physics*, Holt, Rinehart and Winston (Philadelphia, 1976).
- [15] G. Renaud, private information.
- [16] X. J. Chen, A. C. Levi and E. Tosatti, Il Nuovo Cimento **13 D**, 919 (1991).